HOLOGIC®
The Science of Sure

Powerful images. **Clear answers.**

Manage Patient's concerns about Atypical Femur Fracture*

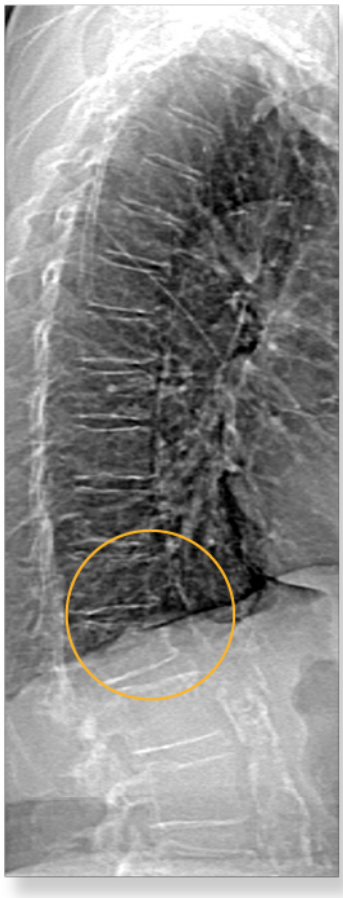

Vertebral Fracture Assessment – a critical part of a complete fracture risk assessment

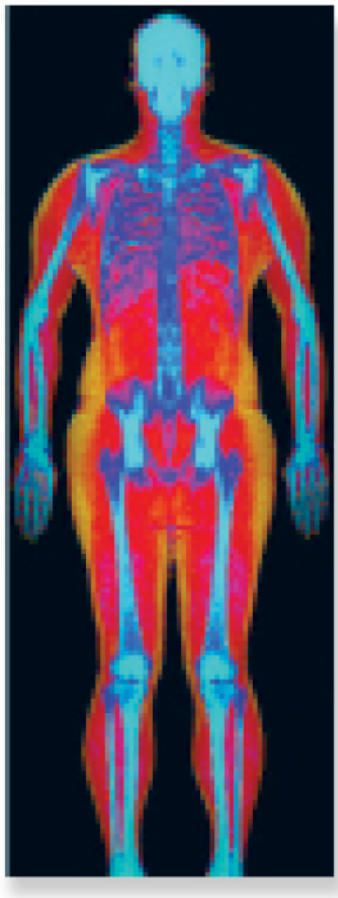

Advanced Body Composition® Assessment – the power to see what's inside

Contact your Hologic rep today at BSHSalesSupportUS@hologic.com

*Incomplete Atypical Femur Fractures imaged with a Hologic densitometer, courtesy of Prof. Cheung, University of Toronto

www.hologic.com | dxaperformance.com | 1.800.442.9892

ORIGINAL ARTICLE

JBMR®

LIGHT/TNFSF14 Promotes Osteolytic Bone Metastases in Non-small Cell Lung Cancer Patients

Giacomina Brunetti,[1] Dimas C Belisario,[2] Sara Bortolotti,[3] Giuseppina Storlino,[3] Graziana Colaianni,[3] Maria F Faienza,[4] Lorenzo Sanesi,[3] Valentina Alliod,[5] Lucio Buffoni,[5] Elisa Centini,[2] Claudia Voena,[2,6] Roberta Pulito,[2] Silvia Novello,[6] Giuseppe Ingravallo,[7] Rita Rizzi,[7] Giorgio Mori,[8] Janne E Reseland,[9] Carl F Ware,[10] Silvia Colucci,[1] Riccardo Ferracini,[11] Maria Grano,[3†] and Ilaria Roato[2†]

[1]Department of Basic and Medical Sciences, Neurosciences and Sense Organs, Section of Human Anatomy and Histology, University of Bari, Bari, Italy
[2]Center for Experimental Research and Medical Studies (CeRMS), A.O.U. Città della Salute e della Scienza di Torino, Turin, Italy
[3]Department of Emergency and Organ Transplantation, Section of Human Anatomy and Histology, University of Bari, Bari, Italy
[4]Department of Biomedical Science and Human Oncology, University of Bari, Bari, Italy
[5]Department of Oncological Sciences, University of Turin Medical School, Turin, Italy
[6]Department of Molecular Biotechnology and Health Sciences, University of Turin, Turin, Italy
[7]Department of Emergency and Organ Transplantation, University of Bari, Bari, Italy
[8]Department of Clinical and Experimental Medicine, University of Foggia, Foggia, Italy
[9]Department of Biomaterials, Institute for Clinical Dentistry, University of Oslo Blindern, Oslo, Norway
[10]Infectious and Inflammatory Disease Center, Sanford Burnham Prebys Medical Discovery Institute, La Jolla, CA, USA
[11]Department of Surgical Sciences (DISC), Orthopaedic Clinic-IRCCS, A.O.U. San Martino, Genoa, Italy

ABSTRACT

Tumor necrosis factor superfamily member 14 (*TNFSF14*), LIGHT, is a component of the cytokine network that regulates innate and adaptive immune responses, which promote homeostasis of lymphoid organs, liver, and bone. Metastatic tumors often disrupt the tissue microenvironment, thus altering the homeostasis of the invaded organ; however, the underlying mechanisms required further studies. We investigated the role of LIGHT in osteolytic bone disease induced by metastatic non-small cell lung cancer (NSCLC). Patients diagnosed with NSCLC bone metastasis show significantly higher levels of LIGHT expressed in monocytes compared with non-bone metastatic tumors and healthy controls. Serum LIGHT levels were also higher in patients with bone metastases than in controls, suggesting a role for LIGHT in stimulating osteoclast precursors. In bone metastatic patients, we also detected increased RNA expression and serum RANKL levels, thus by adding anti-LIGHT or RANK–fragment crystallizable region (RANK-Fc) in PBMC cultures, a significant inhibition of osteoclastogenesis was observed. To model this observation in mice, we used the mouse lung cancer cell line LLC-1. After intratibial implantation, wild-type mice showed an increased number of osteoclasts but reduced numbers of osteoblasts and decreased osteoid formation. In contrast, *Tnfsf14*$^{-/-}$ mice showed no significant bone loss or other changes in bone homeostasis associated with this model. These data indicate LIGHT is a key control mechanism for regulating bone homeostasis during metastatic invasion. Thus, LIGHT may be a novel therapeutic target in osteolytic bone metastases. © 2019 American Society for Bone and Mineral Research.

KEY WORDS: BONE METASTASIS; LIGHT (*TNFSF14*); NON-SMALL CELL LUNG CANCER (NSCLC); OSTEOCLAST

Introduction

Lung cancer represents the primary cause of cancer-related mortality worldwide.[1] The predominant form of lung cancer is non-small cell lung cancer (NSCLC), which metastasizes to bone in 30% to 40% of patients, resulting in a very poor prognosis and median survival time measured in months following lesion detection.[2] NSCLC bone metastases are mainly osteolytic and dramatically impact patients' quality of life, causing morbidity and having substantial financial implications for healthcare providers.[3] In order to develop innovative strategies to inhibit metastatic tumors, we need to identify molecules that regulate bone metastasis.

Received in original form June 10, 2019; revised form December 3, 2019; accepted December 8, 2019. Accepted manuscript online December 11, 2019.
Address correspondence to: Giacomina Brunetti, PhD, Department of Basic and Medical Sciences, Neurosciences and Sense Organs, Section of Human Anatomy and Histology, University of Bari, Piazza Giulio Cesare, 11, 70124 Bari, Italy. E-mail: giacomina.brunetti@uniba.it
Additional Supporting Information may be found in the online version of this article.
[†]MG and IR contributed equally to this work.
Journal of Bone and Mineral Research, Vol. 35, No. 4, April 2020, pp 671–680.
DOI: 10.1002/jbmr.3942

Cancer stem cells have been revealed to play an important role in initiating the metastatic process[4] due to their interaction with the bone microenvironment and immune system.[5] Indeed, the role of the immune system in promoting NSCLC bone metastases has been reported.[6] Among the immune mediators of bone metastases, the immunostimulatory cytokine, LIGHT, a member of TNF superfamily (*TNFSF14*), may be relevant.[7,8] LIGHT is homologous to lymphotoxins and engages the herpes virus entry mediator (HVEM) and the Lymphotoxin-β receptor. LIGHT is produced by immune cells, particularly by activated T-cells, monocytes, natural killers, and neutrophils. It has been reported that LIGHT is involved in increased bone resorption activity typical of the bone diseases,[9,12] such as erosive rheumatoid arthritis[9] (RA) and multiple myeloma.[9,12] LIGHT synergizes with RANKL to stimulate osteoclastogenesis[10–12] and alternately inhibits osteoblastogenesis in myeloma,[12] thus suggesting that high LIGHT levels are harmful for bone. Recently, a study using mice genetically deficient in LIGHT (*Tnfsf14*$^{-/-}$) showed cancellous bone loss, indicating that LIGHT mediates bone homeostasis.[13] Additional evidence has shown that LIGHT expression in T cells and B cells impacts bone homeostasis through the reduced expression of osteoprotegerin (OPG) with consequent increased osteoclastogenesis, thus identifying a mechanism that contributes to the interplay between bone and the immune system.[13] Given this evidence in bone homeostasis, we investigated LIGHT in the malignant bone invasion induced by NSCLC.

Patients and Methods

Patients

Peripheral blood (PB) samples were obtained from 61 newly diagnosed NSCLC patients (37 without bone metastases and 24 with bone metastases) and 13 healthy donors. The patients' characteristics are reported in Supplementary Table 1. Patients signed informed consent according to the Declaration of Helsinki and were approved by the Comitato Etico Interaziendale of A.O.U. Città della Salute e della Scienza di Torino – A.O. Ordine Mauriziano A.S.L. TO1 and of A.O.U. San Luigi Gonzaga di Orbassano.

Flow cytometry analysis

Peripheral blood mononuclear cells (PBMCs) were isolated from PB samples and were stained with the following conjugated antibodies: phycoerythrin (PE) Light (R&D Systems, Inc., Minneapolis, MN, USA), FITC-CD14 (Millipore, Billerica, MA, USA), FITC-CD25, allophycocyanin (APC)-CD4 (Caltag Medsystems, Buckingham, UK), APC-CD8 (GenWay Biotech, San Diego, CA, USA), peridinin-chlorophyll-protein complex (PerCP)-CD16 (BioLegend, San Diego, CA, USA). Unstained samples and isotypic control antibodies PE, FITC, APC, and PerCP-Mouse IgG1, PE-IgG2a (BioLegend; and Miltenyi Biotec, Bergisch Gladbach, Germany) were used as negative controls. Samples were analyzed by flow cytometry with FACs Calibur (Becton Dickinson, Franklin Lakes, NJ, USA) and Flowlogic software (Miltenyi Biotec).

Osteoclastogenesis

PBMCs were isolated after centrifugation over a density gradient using the Ficoll method. PBMCs were plated in 96-well plates at 5×10^5 cell/well, using Alpha-Minimal Essential Medium (α-MEM, supplied by Invitrogen, Carlsbad, CA, USA), supplemented with 10% fetal bovine serum, benzylpenicillin (100 IU/mL) and streptomycin (100 mg/mL) (Lonza, Basel, Switzerland) and maintained at 37°C in a humidified atmosphere of 5% CO_2. To obtain fully differentiated human osteoclasts (OCs), PBMCs from patients with non-bone metastases were cultured in the presence or absence of recombinant human M-CSF (25 ng/mL) and RANKL (30 ng/mL; PeproTech, Rocky Hill, NJ, USA) for 15 days. PBMCs from patients with bone metastases were maintained in α-MEM without any factors, because they spontaneously differentiated into OCs, as described.[14] A neutralizing anti-LIGHT mAb (R&D Systems, Inc.) was added in cultures at 100 and 500 ng/mL twice weekly. PBMCs were cultured in 96-well plates (5×10^5 cells/well) in the presence of RANK–fragment crystallizable region (RANK-Fc) at 20 ng/mL (PeproTech). At the end of the culture period, cells were stained for tartrate-resistant acid phosphatase (TRAP; kit was supplied by Sigma-Aldrich, St. Louis, MO, USA) and OCs were identified as TRAP-positive multinucleated cells containing three or more nuclei.

Osteoblastogenesis

Primary human mesenchymal stem cells (MSCs) from human exfoliated deciduous teeth (SHED), were obtained according to the published procedure.[15] Cells were seeded in 24-well-plates at 400/well, cultured alone or in co-cultures with PBMCs (5.5×10^5 cell/well) in osteogenic differentiating medium, in the absence or presence of 100 ng/mL anti-LIGHT mAb. At the end of culture period (14 days), alkaline phosphatase (ALP) staining (ALP kit was supplied by Sigma-Aldrich) was performed and the ALP-positive osteoblastic colony-forming units (CFU-OB) were counted, as well as the relative percentage of CFU-OB to the total culture area.

Real-time analysis

Total RNA was extracted by Trizol system (Invitrogen) from patients' PBMC samples, and 1 μg of RNA was converted into single-stranded cDNA using the High-Capacity cDNA Reverse Transcription Kit (Applied Biosystems, Foster City, CA, USA). Quantitative real-time PCR was carried out using *SsoAdvanced* Universal SYBR Green Supermix and CFX96 system (Bio-Rad Laboratories, Hercules, CA, USA). The mRNA expression of DcR3, LTβR, HVEM, OPG, and RANKL was evaluated. The β-Actin gene was used as the reference gene. Sequences of the probes and primers were as published.[16]

ELISA

Patients' sera were evaluated for the presence of circulating LIGHT, OPG (R&D Systems, Inc.), and RANKL (BioVendor LLC, Asheville, NC, USA), according to the manufacturer's instructions. The results were expressed as mean ± SD.

Retrovirus preparation and cell transduction

Retroviruses were generated by transfecting the Pallino vector expressing green fluorescent protein (GFP) in the 293GP packaging cell line (Invitrogen). Transfected cells were incubated at 37°C, and supernatants containing viral particles were collected after 24 and 48 hours. For retroviral transduction, 300 μL filtered retroviral supernatants was used to transduce 10×10^4 (1×10^5) mouse Lewis lung carcinoma cell lines (LLC-1; purchased from CLS Cell Lines Service GmbH, Eppelheim, Germany) plated on six-well plates along with polybrene (8 μg/mL). After 12 hours of incubation, 1 mL complete medium was added, and cells were cultured for an additional 48 hours. Transduced cells were then

analyzed for GFP expression using a FACSCalibur flow cytometer (Becton Dickinson). The CELLQuest software (Becton Dickinson) was used for data acquisition and analysis.

Immunohistochemistry and histological analysis on human bone biopsies

Immunohistochemistry was performed on 14 patients' NSCLC bone biopsies fixed in 10% neutral buffered formalin and decalcified with EDTA. These samples were kindly provided by Prof. Papotti from the archive of the Department of Pathology of Città della Salute e della Scienza di Torino. Tissues were embedded in paraffin, and sections were deparaffinized, rehydrated through graded alcohols, and subjected to antigen retrieval for immunohistochemistry. Sections were stained for H&E and polyclonal anti-human LIGHT (Sigma-Aldrich; cat.n. HPA012700).

Mouse model

Tnfsf14 heterozygous mice were kindly provided by author CFW. GFP-conjugated LLC1 (LLC1-GFP) cells were injected intratibially in 6-week-old, female WT and *Tnfsf14*−/− mice. In detail, mice were anesthetized, and 1×10^4 LLC1-GFP cells in 50 μL PBS were injected into the right tibia. PBS (50 μL) was injected into the left tibia for an internal control, as reported in the literature.[17] Four to five animals were housed in single cage at 23°C on a light/dark cycle and were fed a standard rodent chow. After 14 days mice were euthanized and their tissues were surgically excised. Tibias were fixed with 4% (vol/vol) paraformaldehyde for 18 hours at 4°C and processed for micro–computed tomography (μCT) and histological analysis. This animal interventional study is in accordance with the European Law Implementation of Directive 2010/63/EU and all experimental protocols were reviewed and approved by the Veterinary Department of the Italian Ministry of Health.

μCT analysis of tibias

μCT scanning was used to measure morphological indices of metaphyseal tibia regions. Tibias were rotated around their long axes, and images were acquired using Bruker Skyscan 1172 (Kontich, Belgium) with the following parameters: pixel size = 5 μm; peak tube potential = 59 kV; X-ray intensity = 167 μA; 0.4° rotation step. A set of three hydroxyapatite (HA) phantoms were scanned and used for calibration to compute volumetric BMD. For cortical bone properties, tibias were scanned at the mid-diaphysis starting 5.5 mm from proximal tibial condyles and extending for 200 6-μm slices (1.2 mm). For trabecular bone, tibias were scanned starting at 1.9 mm from the proximal tibial condyles, just distal to the growth plate, in the direction of the metaphysis, and extending for 200 slices (1.2 mm).

Histological analysis

For evaluation of the tumor burden, mouse tibias were decalcified and embedded with paraffin. Section were stained with H&E and tumor burden was evaluated as the ratio of tumor area on total area. Microphotographs were captured under a microscope (Leica, Wetzlar, Germany) using a 10× objective lens and analyzed using ImageJ software (NIH, Bethesda, MD, USA; https://imagej.nih.gov/ij/).

For bone histomorphometry, tibias were embedded with methylmethacrylate (MMA) and cut by a standard microtome (RM 2155; Leica, Heidelberg, Germany) into 5-μm slices for histology as described.[13] For analysis of osteoclasts (OC number per bone perimeter [N.Oc/B.Pm]), bone sections were incubated in TRAP staining solution and then counterstained with methyl green; for osteoblast analysis (OB number per bone perimeter [N.Ob/B.Pm]), bone sections were stained with toluidine blue. Goldner's Masson trichrome stain was used to analyze new osteoid formation. Microphotographs were captured under a microscope (Leica) using a 40× objective lens and analyzed using ImageJ software.

Statistical analyses

Statistical analyses were performed by Student's *t* test, nonparametric tests (Mann-Whitney for not normal data), or ANOVA, according to the Statistical Package for the Social Sciences software (IBM SPSS, Armonk, NY, USA). Results were considered statistically significant at $p < .05$.

Results

Increased LIGHT expression in monocytes and serum from patients with NSCLC bone metastases

Through flow cytometry, we analyzed LIGHT expression in CD4 and CD8 T cells, CD14 monocytes, and CD16 neutrophils from 58 of 61 NSCLC patients enrolled in the study: 22 patients with and 36 without bone metastases, and 13 healthy donors. A significantly higher expression of LIGHT was detectable in monocytes from bone metastatic patients compared with non-bone metastatic NSCLC and healthy donors. (Fig. 1*A*–*C*). LIGHT expression by monocytes was higher in patients with metastatic bone lesions than in non-bone metastatic ones (66.5 ± 24.5 versus 43.3 ± 25.2, $p = .001$), healthy donors (66.5 ± 24.5 versus 8.5 ± 4.6, $p = .0002$) and in non-bone metastatic patients than in healthy donors (43.3 ± 25.2 versus 8.5 ± 4.6, $p = .0001$) (Fig. 1*D*). Activated CD4/CD25 T cells express higher levels of LIGHT compared to CD8 T cells but were similar across all groups; no differences were evident among the other cellular subsets. The mean values of LIGHT expression among the different PBMC subpopulations is reported in Supplementary Table 2. Serum LIGHT levels were also significantly higher in bone metastatic patients than in non-bone metastatic ones (186.8 ± 191.2 pg/mL versus 115.8 ± 73 pg/mL, $p = .04$) and healthy donors (186.8 ± 191.2 pg/mL veruss 85.7 ± 38.4 pg/mL, $p = .04$) (Fig. 1*E*). Because LIGHT action is mediated by the interaction with its receptors, lymphotoxin-β receptor (LTβR), herpesvirus entry mediator (HVEM), and decoy receptor 3 (DcR3), we also evaluated their expression on patients' PBMCs. LTβR was not expressed, whereas HVEM and DcR3 expression was not significantly different between bone and non-bone metastatic patients (data not shown).

LIGHT expression in NSCLC bone metastases

In our series of bone metastasis, careful routine histopathological analysis showed atypical epithelial neoplastic cells morphologically consistent with NSCLC within hematopoietic tissue, without evident malignant phenotype. In particular, we investigated the expression of LIGHT in 14 NSCLC metastatic bone biopsies by immunostaining. We found 8 of 14 tumor epithelial cell cases expressed LIGHT, regardless the absence (Fig. 2*A*; ie, early phase of bone marrow colonization) or presence of a reactive background, such as fibrous tissue (Fig. 2*B*) and osteosclerosis (Fig. 2*C*). Notably, cytoplasmic staining of LIGHT was intermediate or strong in bone metastases with no gland forming (ie, solid) NSCLCs, whereas it was minimal or negative in NSCLCs

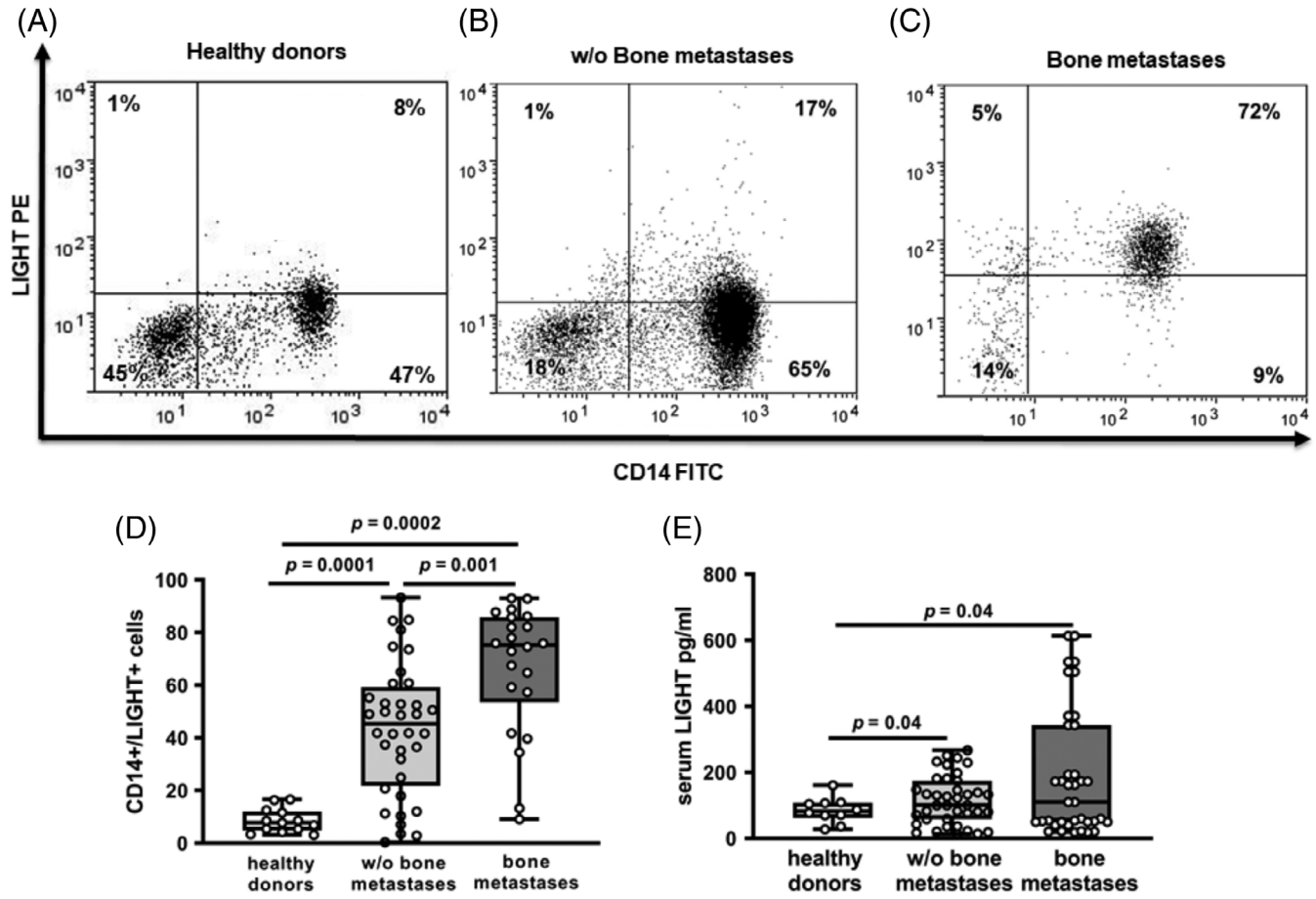

Fig. 1. LIGHT expression in monocytes and serum from NSCLC patients. (*A–C*) Representative dot plots of CD14+/LIGHT+ monocytes from healthy donors and patients without or with bone metastases are shown. (*D*) Significant increase of LIGHT expression on CD14+ cells derived from patients without or with bone metastases compared to healthy donors, and from patients with bone metastases compared to non-bone metastatic ones. (*E*) Increased serum LIGHT levels in patients without and with bone metastases with respect to healthy donors. Comparison of multiple means was performed by one-way ANOVA; *p* values as shown.

associated with a gland-forming component (Fig. 2*D*). The LIGHT expression was not detected in hematopoietic tissue.

LIGHT blockade inhibits osteoclastogenesis in vitro

As described,[6,14] OCs formed spontaneously in PBMC cultures from bone metastatic patients, whereas cells from non-bone metastatic patients required M-CSF and RANKL. The number of OCs in cultures from patients with bone metastases was significantly higher than those from non-bone metastatic cultures, even though these ones received stimulating factors (272 $\pm$ 98; 131 $\pm$ 49, $p = .002$), (Fig. 3*A*). A neutralizing mAb to LIGHT added to OC cultures of both bone and non-bone metastases inhibited osteoclastogenesis, but the decrease was statistically significant only for bone metastatic patients (272 $\pm$ 98 versus 132 $\pm$ 74, $p = .01$) (Fig. 3*B*). The significant inhibition of osteoclastogenesis in bone metastatic patients was also confirmed by TRAP staining (Fig. 3*B*). In PBMC cultures from non-bone metastases, osteoclastogenesis was only slightly reduced. Indeed, in these patients, LIGHT expression was less than in bone metastatic patients, suggesting that only high levels of LIGHT can affect osteoclastogenesis in vitro.

RANKL and OPG in NSCLC patients

LIGHT synergizes with RANKL to induce osteoclastogenesis,[9,12] and spontaneous osteoclastogenesis in bone metastatic patients is regulated by RANKL.[6,14] The detection of higher LIGHT expression in patients with bone metastases suggests that the effect of LIGHT on osteoclastogenesis might be due to a contribution from RANKL. We found serum RANKL levels significantly higher in these patients than in non-bone metastatic ones (17.6 $\pm$ 21.2 ng/mL versus 6.5 $\pm$ 2.8 ng/mL, respectively). By contrast, serum OPG levels were the same between the two groups (2 $\pm$ 0.8 ng/mL versus 1.9 $\pm$ 0.6 ng/mL, respectively). However, the RANKL/OPG ratio significantly increased in patients with bone metastases compared to non-bone ones (8.9 $\pm$ 10 ng/mL versus 6.8 $\pm$ 7.2 ng/mL, respectively, $p = .04$, Fig. 3*C*). After analyzing RANKL and OPG mRNA expression in PBMCs, we found the same trend as for serum levels, but the difference was not statistically significant (1.2 $\pm$ 0.4 versus 0.9 $\pm$ 0.3, respectively, Fig. 3*D*). The significant RANKL increase in patients with bone compared to non-bone metastases prompted us to test RANK-Fc on PBMC cultures from bone metastatic patients to demonstrate its ability to inhibit OC formation (Fig. 3*E*), thus suggesting RANKL involvement in osteoclastogenesis.

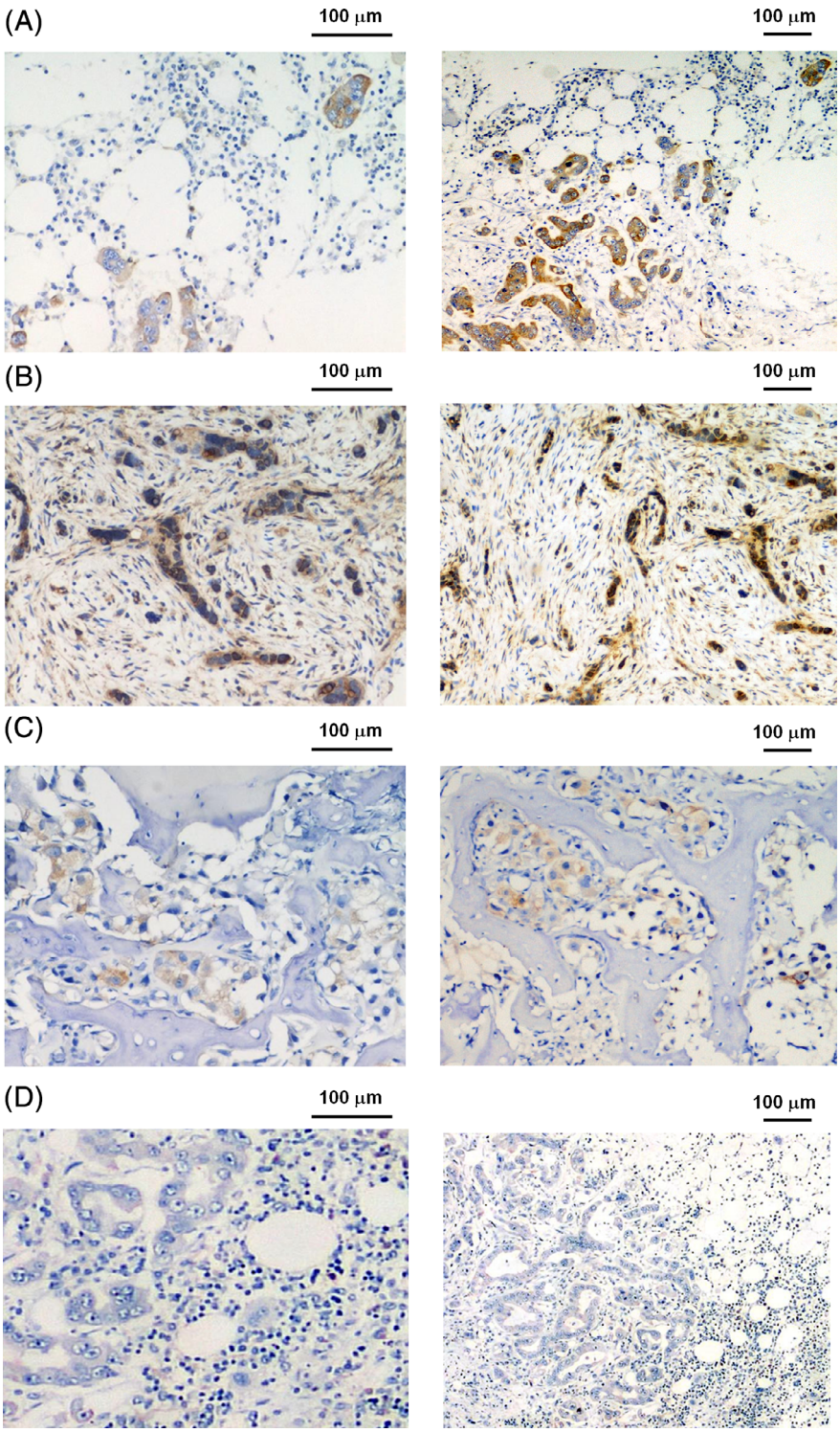

Fig. 2. LIGHT expression in NSCLC bone metastases. LIGHT detected in tumor epithelial cells, regardless of the absence (*A*, *D*) or presence of a reactive background, such as fibrous tissue (*B*) and osteosclerosis (*C*). (*D*) Cytoplasmic staining of LIGHT is minimal or negative in NSCLCs associated with a gland-forming component. As it can be seen, in *A* and *D* it is also clear of hematopoietic tissue, whereas in *B* and *C* the carcinomatous infiltration is massive without residual bone marrow. Photomicrographs on the right: original magnification ×100; photomicrographs on the left: original magnification ×200.

Blockade of LIGHT does not affect osteoblastogenesis

We investigated whether LIGHT mediates osteoblastogenesis in co-cultures stimulated by NSCLC PBMCs, because it was revealed to be able to inhibit CFU-OB formation in multiple myeloma.[12] Although PBMCs stimulate MSC proliferation, LIGHT released by PBMCs could interfere with CFU-OB, so we added anti-LIGHT to counteract this potential inhibition. We performed co-cultures

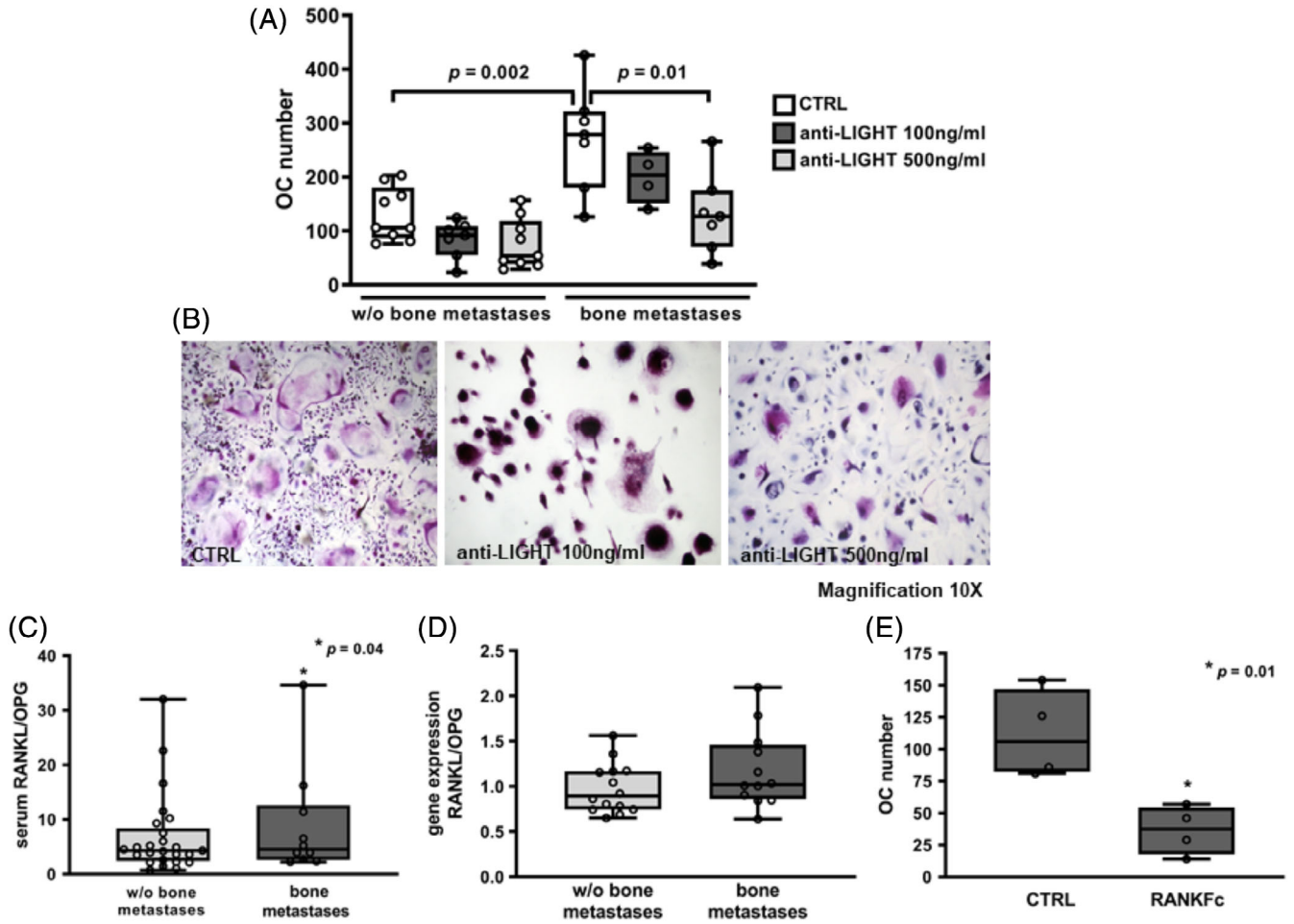

Fig. 3. LIGHT and RANKL in the regulation of osteoclastogenesis in vitro. (*A*) Increased number of multinucleated (>3 nuclei), TRAP-positive OCs in bone metastatic patients compared to non-bone metastatic ones, and reduced OC number in bone metastatic patients after anti-LIGHT treatment (500 ng/mL). Comparison of multiple means was performed by one-way ANOVA. (*B*) Representative images of TRAP staining for OCs derived from bone metastatic patients, in absence (CTRL) or presence of 100 and 500 ng/mL of anti-LIGHT. Increased RANKL/OPG ratio in patients with bone metastases compared to non-bone ones (*C*); gene expression analysis, reported as RANKL/OPG ratio (*D*); significant reduction in osteoclastogenesis in PBMC cultures treated with RANK-fc (20 ng/mL) (*E*). Two-tailed unpaired *t* tests were conducted for serum level and gene expression of RANKL/OPG, two-tailed paired *t* test was conducted for RANK-fc experiments; *p* values as shown. Magnification ×10.

of SHED-MSCs with PBMCs from patients with both bone and non-bone metastases in osteogenic medium, with or without 100 ng/mL of anti-LIGHT mAb (Fig. 4). Anti-LIGHT did not affect CFU-OB formation in co-cultures of patients with non-bone or bone metastases, as shown by ALP staining (Fig. 4*A*,*B*, respectively). We observed decreased CFU-OB formation in patients with bone metastases compared to non-bone metastases, even though the difference was not statistically significant (Fig. 4*C*). These data support the known defect in OB formation and activity in the presence of osteolytic bone metastases.

Tnfsf14$^{-/-}$ mice injected with LLC1 are protected from bone loss

To evaluate in vivo the effect of LIGHT neutralization, we injected intratibial WT and *Tnfsf14*$^{-/-}$ (KO) mice with the murine Lewis lung cancer cell line LLC-1. Interestingly, in tibias the tumor burden, measured by histologic analysis showed a slight reduction of tumor area in KO bones with respect to WT mice (Fig. 5*A*-*C*). Furthermore, quantitative observations of μCT-generated section images of tibias (Fig. 6) showed a significant decrease in trabecular bone mass in injected WT mice (WT-injected) compared to the vehicle WT mice (WT-vehicle) (Fig. 6*A*,*B*). Interestingly, no significant differences were observed between KO-injected mice and the KO-vehicle (Fig. 6*C*,*D*), as well as for WT-injected versus KO-injected mice (Fig. 6*B*–*D*), notwithstanding a reduction trend. In particular, the WT-injected mice showed significantly reduced BV/TV, Tb.N, Tb.Th, and Tb.Sp compared to the WT-vehicle mice (Fig. 6*E*–*H*). Otherwise, these parameters did not show significant variation in KO-injected mice toward the vehicle or in WT-injected mice versus KO-injected mice. We consistently found a significant increase in TRAP-stained OC number per bone perimeter observed only in WT-injected mice versus the WT-vehicle mice (Fig. 7*A*). Significantly, a slight decrease in OB cell numbers was measured in WT-injected mice compared

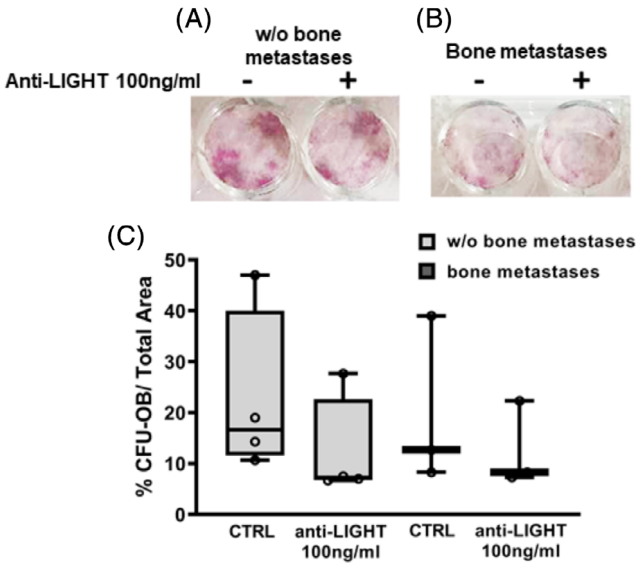

Fig. 4. LIGHT does not affect osteoblastogenesis in co-cultures of SHED-MSCs and patients' PBMCs. Representative image of ALP staining for CFU-OB in co-cultures of patients without bone metastases (*A*) and with bone metastases (*B*), in absence or presence of 100 ng/mL anti-LIGHT neutralizing mAb. (*C*) The mean number of CFU-OB/total area was not different in presence or absence of anti-LIGHT for both bone and non-bone metastatic patients. Data are derived from cultures of four non-bone metastatic patients and three bone metastatic ones. Two-tailed paired *t* tests were performed on both bone and non-bone metastatic groups; *p* values as shown. Magnification ×10.

to WT-vehicle mice (Fig. 7*B*). Otherwise, there were no significant differences between KO-injected and KO-vehicle mice as well as for WT-injected and KO-injected mice (Fig. 7*B*). Furthermore, a ~52% reduction in the area of osteoid surface to bone surface (OS/BS) was observed in WT-injected mice compared to the WT-vehicle mice ($p < .001$), whereas in KO-injected mice, a slight OS/BS% decrease was observed, not statistically significant compared to the KO-vehicle mice (Fig. 7*C*). OS/BS% detected between WT-injected and KO-injected mice did not show any significant difference (Fig. 7*C*). Overall, our data suggest that LIGHT deficiency protects the loss of bone associated with LLC1 tumor cells.

Discussion

In this study, we showed for the first time that, in patients with bone metastases from NSCLC, LIGHT expression increased in circulating monocytes compared to patients without bone metastases. Previously, it was reported that multiple myeloma patients with bone disease showed an increased expression of LIGHT in both CD14+ monocytes and CD16+ neutrophils,[12] together with the role played by LIGHT in regulating osteoclastogenesis. Both NSCLC and multiple myeloma are characterized by osteolytic bone disease, so increased LIGHT expression from monocytes (which can differentiate into OCs) suggests that LIGHT is also involved in the pathogenesis of osteolytic bone metastases from NSCLC. During the analysis of LIGHT expression in CD4+ and CD8+ T cells, as well as CD16+ neutrophils, we found higher expression in CD4/CD25+ cells than CD8+ T cells, although no difference was seen between bone and non-bone metastatic patients. This suggests that LIGHT expressed in CD4 T cells could stimulate OC formation, as well as other factors

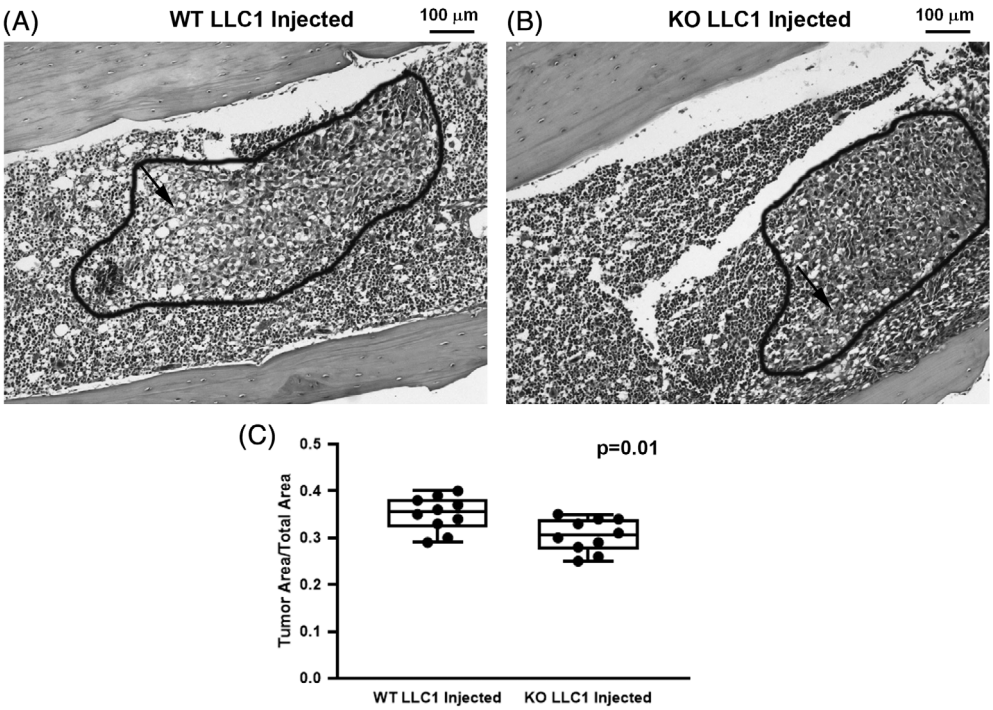

Fig. 5. *Tnfsf14*−/− mice display decreased tumor burden in bone. Representative H&E-stained sections from WT (*A*) and KO (*B*) tibias injected with Lewis lung carcinoma cell lines (LLC-1). (*C*) Graphs show calculated histologic analysis of tumor area/total bone area for WT and KO-injected mice, a slight decrease in tumor area in KO bones respect to WT-mice was evident. Arrows point to tumor cells. The marked area represents the tumor area. $n = 10$ mice per group. Two-tailed paired *t* tests were performed; *p* value as shown.

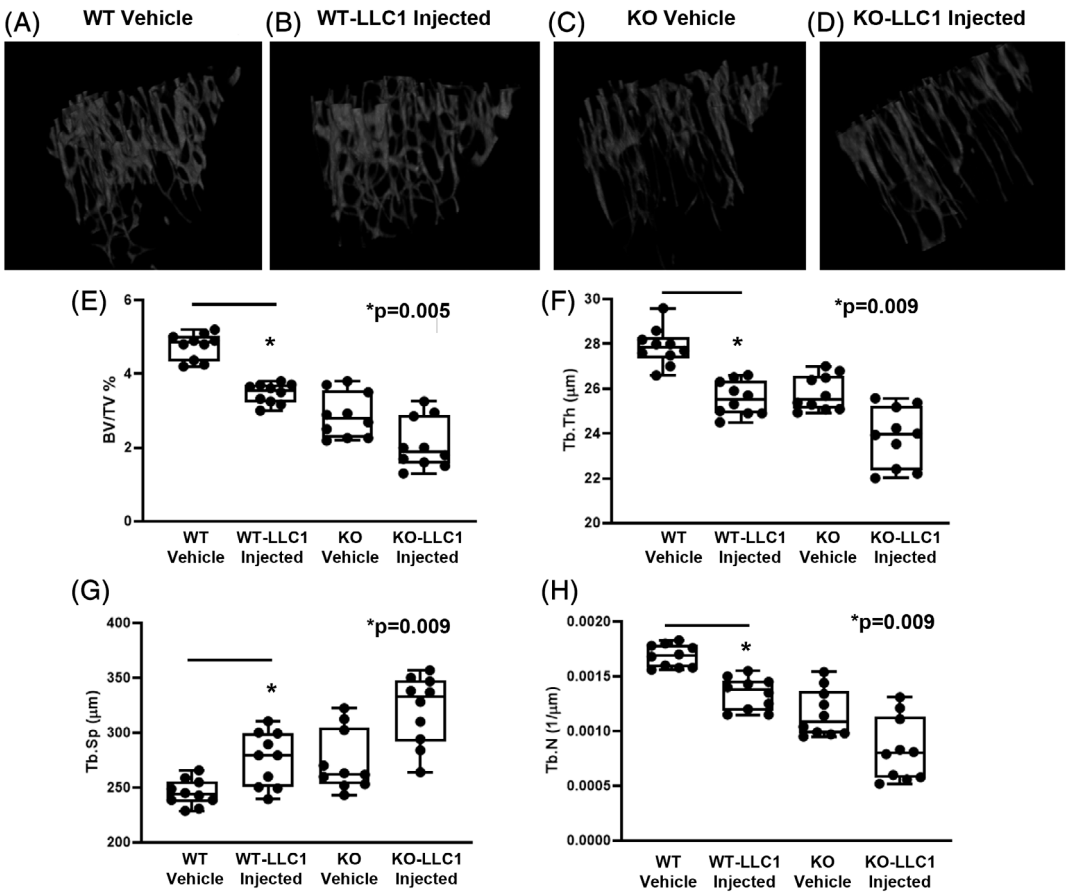

Fig. 6. *Tnfsf14*$^{-/-}$ mice injected with LLC1 are protected from bone loss. (*A–D*) Representative μCT-generated section images of trabecular bone in tibias harvested from WT and *Tnfsf14*$^{-/-}$ mice, previously injected with vehicle or Lewis lung carcinoma cell lines (LLC-1). (*E–H*) Graphs show calculated trabecular parameters at the metaphysis of WT and *Tnfsf14*$^{-/-}$ mice. Trabecular bone parameters included BV/TV, Tb.Th, Tb.N, and Tb.Sp. The WT-injected mice displayed significantly reduced BV/TV, Tb.N, Tb.Th, and Tb.Sp compared to the WT-vehicle mice. These parameters did not show significant variation for KO-injected mice with respect to the vehicle or for WT-injected mice versus KO-injected mice. $n = 10$ mice per group. Comparison of multiple means was performed by one-way ANOVA; p values as shown. BV/TV = bone volume/total volume; Tb.Th = trabecular thickness; Tb.N = trabecular number; Tb.Sp = trabecular separation.

(ie, IL-7, RANKL, TNF) released by CD4 T cells, known to promote osteoclastogenesis.[18,19]

LIGHT production is reflected in the serum concentration; indeed, it was significantly increased in NSCLC bone metastatic patients, suggesting that LIGHT might regulate systemic osteolysis by activating circulating OC precursors.

NSCLC bone biopsies showed distinctive LIGHT expression in bone metastases. Specifically, the LIGHT staining in the samples was markedly associated with less-differentiated cancer cells, whereas only minimal or negative expression was detected where intraosseous neoplastic cells were organized in a gland-forming pattern, this being considered a histopathological detail of nonaggressive behavior. This pattern of staining could reflect the association of LIGHT bound to DcRe, a soluble receptor that binds LIGHT, present in bone and other tissues, and secreted by tumor cells.[20] Consequently, we advocated a new perspective in studying the role of LIGHT in NSCLC cells by considering their differentiation status. In fact, as reported with reference to a model of colon cancer, enforced LIGHT expression in tumor cells triggered regression of established tumors and slowed metastatic formation due to LIGHT stimulating an anti-tumor response.[21,22] Our finding about the variation of LIGHT expression, according to the differentiated status of NSCLC cells, leads us to speculate that NSCLC cells may use a different ability to escape the immune system.

We also confirm the role of LIGHT in sustaining OC formation using an in vitro osteoclastogenesis assay based on patients' PBMC cultures. Specifically, a neutralizing anti-LIGHT antibody inhibited osteoclastogenesis in PBMCs of patients with bone metastases, whereas in PBMC cultures from patients with non-bone metastases, osteoclastogenesis was only slightly reduced. These results suggest that patients without bone metastases expressed LIGHT at physiological levels, which did not affect osteoclastogenesis; namely, the anti-LIGHT did not significantly inhibit OC formation. It has been recently demonstrated that, physiologically, LIGHT interfered with bone homeostasis protecting bone, while the absence of LIGHT caused cancellous bone loss. Truly, LIGHT deficiency is associated with pro-osteoclastogenic stimulation and increased OC bone resorption.[13] To the same degree, elevated LIGHT levels in NSCLC patients can activate osteolytic mechanisms, which is also a function of the RANK/RANKL/OPG axis.[6] Here, we show that adding RANK-Fc to PBMC cultures significantly inhibited osteoclastogenesis in NSCLC patients with bone metastases, suggesting that both RANKL and LIGHT contribute to bone disease.

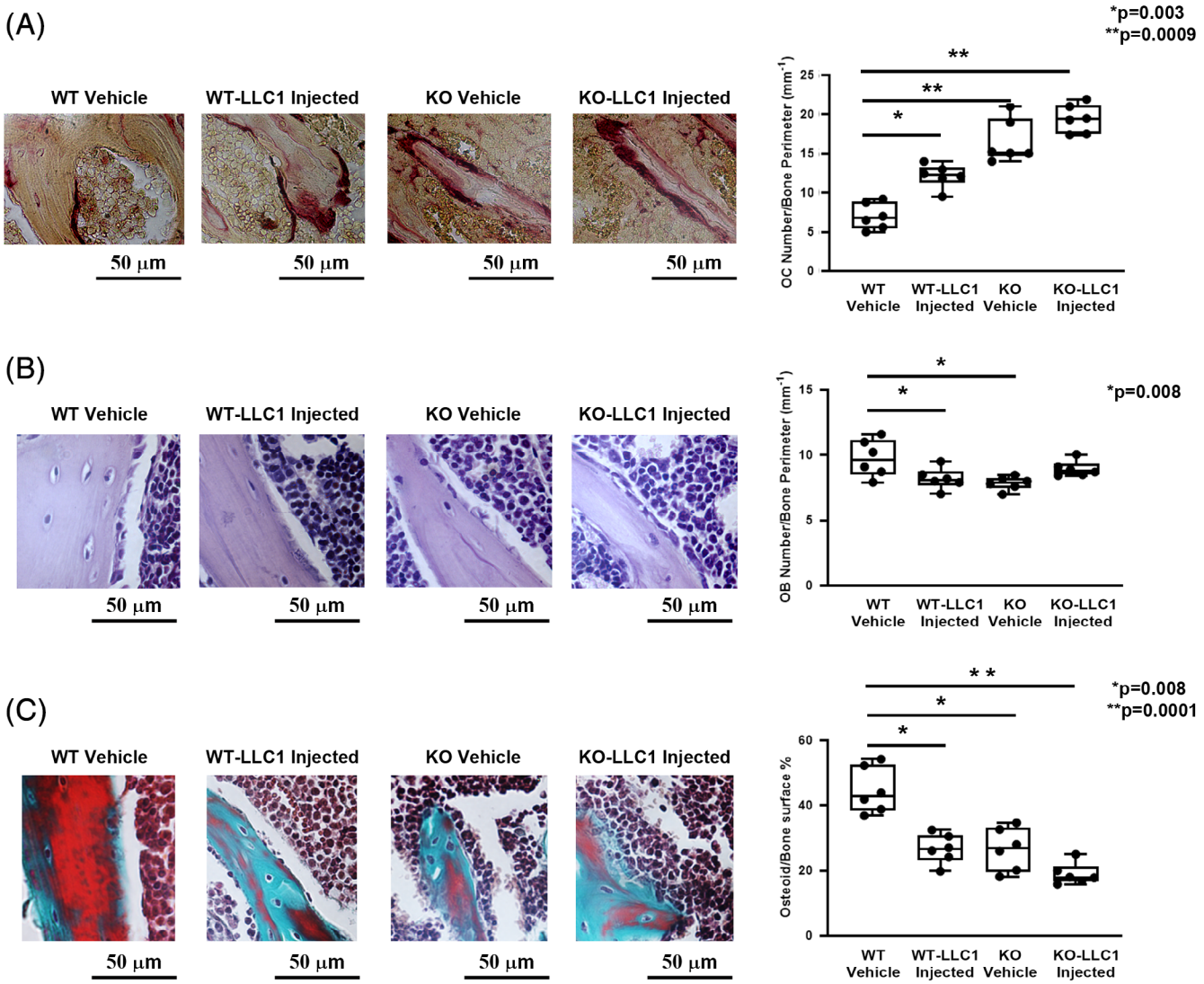

Fig. 7. LIGHT stimulates osteoclastogenesis and inhibits osteoblastogenesis in vivo. Representative images of tartrate-resistant acid phosphatase–stained osteoclasts in tibia sections from WT and *Tnfsf14*$^{-/-}$ mice, injected with vehicle or Lewis lung carcinoma cell lines (LLC-1), together with N.Oc/B.Pm. (*A*) A significant increase in OC number was observed only in WT-injected mice compared to the WT-vehicle mice. (*B*) Toluidine blue–stained osteoblasts in tibial sections from the same mice together with N.Ob/B.Pm. A slight but significant decrease in OB cell numbers was measured in WT-injected mice compared to WT-vehicle. (*C*) Representative images of Goldner's Masson trichrome–stained tibia sections, together with measurement of percentage of osteoid per BS. A significant reduction was observed only in WT-injected mice compared to the WT vehicle mice. $n = 6$ mice per group. Comparison of multiple means was performed by one-way ANOVA; p values as shown. Magnification ×40. N.Oc/B.Pm = OC number per bone perimeter; N.Ob/B.Pm = OB number per bone perimeter; BS = bone surface.

In basal conditions, osteoclastogenesis is mainly regulated by the RANKL/OPG ratio. Here, in our cohort of NSCLC bone metastatic patients, we observed high LIGHT levels and an unbalanced RANKL/OPG ratio in favor of RANKL. Indeed, patients with bone metastases had higher levels of RANKL than non-bone metastatic ones, whereas OPG levels were comparable between the two groups. LIGHT-KO mice also showed an unbalanced RANKL/OPG ratio, due to OPG variations, while RANKL levels did not differ.[13] In patients with osteolytic bone disease as well as in multiple myeloma patients,[23] we detected both high levels of RANKL and LIGHT, which upregulated osteoclastogenesis. Conversely, in *Tnfsf14*−/− mice, OPG increased, but the result was always an unbalanced RANKL/OPG ratio associated with an upregulation of osteoclastogenesis.[13] These data corroborate a fundamental role of LIGHT in the maintenance of skeletal physiology, because its dysregulation causes abnormal osteoclastogenesis.

To study the potential effects of LIGHT on osteoblastogenesis, we co-cultured SHED-derived MSCs and patient PBMCs in the presence or absence of anti-LIGHT antibody. By contrast to LIGHT KO mice and multiple myeloma, we observed no significant LIGHT effect on osteoblastogenesis. We also found decreased CFU-OB formation in patients with bone metastases compared to non-bone ones. Despite this difference not statistically significant, the results support the known defect in OB

formation and activity in the presence of osteolytic bone metastases.[5]

The mouse NSCLC-bone disease model revealed that the tumor burden was reduced in KO bones compared to WT mice. Furthermore, LIGHT deficiency prevented significant decrease in bone mass, whereas increased osteoclastogenesis and decreased osteoblastogenesis occurred in WT mice. Osteoid formation was also significantly reduced only in tumor-bearing WT mice, whereas KO mice showed only a slight reduction, suggesting a key role for LIGHT in causing bone disease in metastatic patients. In KO-LLC1 injected mice, the reduced bone disease may occur because of the decreased tumor burden compared to WT-injected mice. Nevertheless, we cannot exclude that the absence of further bone loss with tumor injection in KO mice might depend on the already low bone mass, associated with the LIGHT KO phenotype. A similar scenario has been described for another co-stimulatory cytokine, CD40L; indeed, mice lacking CD40L do not sustain the acute bone loss triggered by estrogen deficiency.[24]

We reported that *Tnfsf14*−/− mice showed a reduced trabecular bone mass compared to WT mice as well as high levels of LIGHT in different pathologies with osteolytic bone disease, such as multiple myeloma,[12,23] alkaptonuria,[25] chronic kidney disease, and hemodialysis in patients.[26] Moreover, Edwards and colleagues[9] measured increased LIGHT levels in erosive rheumatoid arthritis, thus sustaining its central role in pathological bone remodeling.

In conclusion, the accumulated evidence supports a key role of LIGHT in pathological bone remodeling and suggests that neutralizing LIGHT activity could improve bone loss in patients with NSCLC.

Disclosures

All authors state that they have no conflicts of interest.

Acknowledgments

This work was supported by the CRT and Compagnia di San Paolo Foundations; Fondazione Ricerca Molinette ONLUS (to IR). We thank Dr. Federico Mussano and Prof. Mauro Papotti for providing us SHED-MSCs and NSCLC bone biopsies, respectively. We thank Dr. Norma Origgi for the final english revision and a special thanks to Dr. Mara Compagno for critical discussion of the manuscript.

Authors' roles: GB and IR designed the study, and drafted the manuscript; SB performed histological studies; DCB, EC, and RP: performed experiments on human biological samples; LS performed ELISA, GI performed immunohistochemistry; VA, SN, and LB recruited patients, provided samples and clinical data; CV performed retrovirus preparation and cell transduction; GM performed the statistical analysis; RR and MFF critically revised the clinics; CFW provides mice and critically revised the manuscript; JER provides her expertise in μCT; GC and GS analyzed μCT results; SC and RF critically revised the manuscript; MG supervised all experiments and critically revised the manuscript. All authors read and approved the final manuscript. GB and IR take responsibility for the integrity of the data analysis.

References

1. Bray F, Ferlay J, Soerjomataram I, Siegel RL, Torre LA, Jemal A. Global cancer statistics 2018: GLOBOCAN estimates of incidence and mortality worldwide for 36 cancers in 185 countries. CA Cancer J Clin. 2018;68:394–424.
2. Langer CJ, Besse B, Gualberto A, Brambilla E, Soria JC. The evolving role of histology in the management of advanced non-small-cell lung cancer. J Clin Oncol. 2010;28:5311–20.
3. Delea T, Langer C, McKiernan J, et al. The cost of treatment of skeletal-related events in patients with bone metastases from lung cancer. Oncology. 2004;67:390–6.
4. Bertolini G, D'Amico L, Moro M, et al. Microenvironment-modulated metastatic CD133+/CXCR4+/EpCAM- lung cancer-initiating cells sustain tumor dissemination and correlate with poor prognosis. Cancer Res. 2015;75:3636–49.
5. Roato I, Ferracini R. Cancer stem cells, bone and tumor microenvironment: key players in bone metastases. Cancers (Basel). 2018;10(2):56.
6. Roato I, Gorassini E, Buffoni L, et al. Spontaneous osteoclastogenesis is a predictive factor for bone metastases from non-small cell lung cancer. Lung Cancer. 2008;61:109–16.
7. Mauri DN, Ebner R, Montgomery RI, et al. LIGHT, a new member of the TNF superfamily, and lymphotoxin alpha are ligands for herpesvirus entry mediator. Immunity. 1998;8:21–30.
8. Tamada K, Shimozaki K, Chapoval AI, et al. LIGHT, a TNF-like molecule, costimulates T cell proliferation and is required for dendritic cell-mediated allogeneic T cell response. J Immunol. 2000;164:4105–10.
9. Edwards JR, Sun SG, Locklin R, et al. LIGHT (TNFSF14), a novel mediator of bone resorption, is elevated in rheumatoid arthritis. Arthritis Rheum. 2006;54:1451–62.
10. Ishida S, Yamane S, Nakano S, et al. The interaction of monocytes with rheumatoid synovial cells is a key step in LIGHT-mediated inflammatory bone destruction. Immunology. 2009;128:e315–24.
11. Hemingway F, Kashima TG, Knowles HJ, Athanasou NA. Investigation of osteoclastogenic signalling of the RANKL substitute LIGHT. Exp Mol Pathol. 2013;94:380–5.
12. Brunetti G, Rizzi R, Oranger A, et al. LIGHT/TNFSF14 increases osteoclastogenesis and decreases osteoblastogenesis in multiple myeloma-bone disease. Oncotarget. 2014;5:12950–67.
13. Brunetti G, Faienza MF, Colaianni G, et al. Impairment of bone remodeling in LIGHT/TNFSF14-deficient mice. J Bone Miner Res. 2018;33:704–19.
14. Roato I, Grano M, Brunetti G, et al. Mechanisms of spontaneous osteoclastogenesis in cancer with bone involvement. FASEB J. 2005;19:228–30.
15. Mussano F, Genova T, Petrillo S, Roato I, Ferracini R, Munaron L. Osteogenic differentiation modulates the cytokine, chemokine, and growth factor profile of ASCs and SHED. Int J Mol Sci. 2018;19(5):1454.
16. D'Amelio P, Roato I, D'Amico L, et al. Bone and bone marrow pro-osteoclastogenic cytokines are up-regulated in osteoporosis fragility fractures. Osteoporos Int. 2011;22:2869–77.
17. Wright LE, Ottewell PD, Rucci N, et al. Murine models of breast cancer bone metastasis. Bonekey Rep. 2016;5:804.
18. Horwood NJ, Kartsogiannis V, Quinn JM, Romas E, Martin TJ, Gillespie MT. Activated T lymphocytes support osteoclast formation in vitro. Biochem Biophys Res Commun. 1999;265:144–50.
19. Takayanagi H, Ogasawara K, Hida S, et al. T-cell-mediated regulation of osteoclastogenesis by signalling cross-talk between RANKL and IFN-gamma. Nature. 2000;408:600–5.
20. Cheung TC, Coppieters K, Sanjo H, et al. Polymorphic variants of LIGHT (TNF superfamily-14) alter receptor avidity and bioavailability. J Immunol. 2010;185:1949–58.
21. Qiao G, Qin J, Kunda N, et al. LIGHT elevation enhances immune eradication of colon cancer metastases. Cancer Res. 2017;77:1880–91.
22. Yu P, Lee Y, Liu W, et al. Priming of naive T cells inside tumors leads to eradication of established tumors. Nat Immunol. 2004;5:141–9.
23. Brunetti G, Rizzi R, Storlino G, et al. LIGHT/TNFSF14 as a new biomarker of bone disease in multiple myeloma patients experiencing therapeutic regimens. Front Immunol. 2018;9:2459.
24. Li JY, Tawfeek H, Bedi B, et al. Ovariectomy disregulates osteoblast and osteoclast formation through the T-cell receptor CD40 ligand. Proc Natl Acad Sci U S A. 2011;108(2):768–73.
25. Brunetti G, Tummolo A, D'Amato G, et al. Mechanisms of enhanced osteoclastogenesis in Alkaptonuria. Am J Pathol. 2018;188:1059–68.
26. Cafiero C, Gigante M, Brunetti G, et al. Inflammation induces osteoclast differentiation from peripheral mononuclear cells in chronic kidney disease patients: crosstalk between the immune and bone systems. Nephrol Dial Transplant. 2018;33:65–75.